



e-mail  
Martine.Michou@meteo.fr

# A new version of the CNRM Chemistry-Climate Model, CNRM-CCM: description and improvements from the CCMVal-2 simulations

WCRP Open Science  
Conference  
Denver, USA  
24-28 October 2011

Martine Michou, David Saint-Martin, Hubert Teysse re, Fernand Karcher  
Centre National de Recherches M t orologiques (CNRM), Toulouse, France

## 1. Introduction

Three-dimensional atmospheric circulation models with a fully interactive representation of stratospheric ozone chemistry are known as stratosphere-resolving Chemistry-Climate Models (CCMs). They are key tools for the attribution and projection of stratospheric ozone changes arising from the combined effects of changes in the amounts of greenhouse gases and ozone-depleting substances. We present here results of a modelling activity that lead to the definition and implementation of a new version of the M t o-France CNRM CCM, "CNRM-CCM".

## 2. Description of the CNRM-CCM Model and of the simulations performed

### 2.1 From CNRM-ACM to CNRM-CCM

The new model version CNRM-CCM is an evolution of the previous version CNRM-ACM, largely evaluated in the context of the CCMVal-2 activity, both in terms of their underlying General Circulation Model (GCM), as well as in the way these CCMs deal with the chemistry part through the interactions between chemical, radiative and dynamical processes. A number of minor differences exist between the dynamical/physical components of the CNRM-ACM GCM and that of the CNRM-CCM GCM (ARPEGE-Climat version 5.2). However, a major evolution concerns their radiation scheme, both in the SW spectrum with 2 and 6 bands respectively, and above all in the LW spectrum. A second major difference between CNRM-ACM and CNRM-CCM is that the chemistry of CNRM-CCM is so-called "on-line": the simulation of gaseous chemistry has been directly integrated within the GCM code. Chemical routines are a subset of the entire set of model routines, and chemical species are considered as prognostic variables of the model. The advection scheme is thus the same for meteorological and for chemical variables, avoiding inconsistencies with transport. More details can be found in [Michou et al., GMD, 2011].

### 2.2 Simulations and diagnostics analysed

We analysed a 47-yr transient simulation (1960–2006) defined as the CCMVal-2 REF-B1 simulation. The diagnostics considered appear in Table 1. For further details see [Michou et al., GMD, 2011]

Table 1. Diagnostics considered in this study.

Process	Diagnostics	Variables	Observations
Dynamics	High lat. strat. biases	T (Temperature)	ERA-40 Uppala et al. (2005)
	Winter, spring		ERA-Interim; Simmons et al. (2006)
			NCIP; UKMO reana.; Eyring et al. (2006)
Transport	Easterlies at 60S	U (zonal wind)	ERA-40; ERA-Interim
	SH and NH Night Polar Jet		ERA-40
	Tape recorder	H <sub>2</sub> O	HALOE; Good and Russell (2005)
	Latitu. profiles at 0.5, 10 and 50hPa	Age of air	Vautour; Eyring et al. (2006)
	Vert. and latitu. profiles	CH <sub>4</sub>	HALOE
Seasonal cycles	O <sub>3</sub> , H <sub>2</sub> O	HALOE; MIPAS; SPARC (2010)	
	at 100, 200hPa and at 40° N-60° N, 60° S-40° S	HNO <sub>3</sub>	MIPAS
	Seasonal cycles at 100hPa Equator		
UTLS	Latitu. profiles ANN, DJF, JJA	T	ERA-40; ERA-Interim
	at 100hPa	O <sub>2</sub> , H <sub>2</sub> O	HALOE
Natural variability	Annin. at 90hPa	Trapp, pressure	ERA-40; ERA-Interim
			ERA-Interim
Chemistry	Vert. and latitu. profiles	H <sub>2</sub> O, O <sub>3</sub> , HCl	HALOE
	Time ser. at 50hPa, 80° S	Cl	Vautour; Eyring et al. (2006)
	Seasonal cycles at 50, 10hPa and at 30° N-60° N	CH <sub>4</sub> , H <sub>2</sub> O, O <sub>3</sub> , HCl	HALOE
	at 30° S-60° S, 15° S-15° N	NO <sub>2</sub> , N <sub>2</sub> O <sub>5</sub>	MIPAS
		SCIAMACHY; SPARC (2010)	
		CH <sub>3</sub> NO <sub>2</sub>	MIPAS
		CO	MLS; Lee et al. (2011)
Total column 1980-1990, 1990-2000	O <sub>3</sub>	BS2.7; Bodeker et al. (2005)	

## 3. Results

### 3.1 Overview

As an overall picture of the agreement between the observations and the CNRM model outputs, we plotted a Taylor diagram of all the diagnostics analysed (see Fig.13). Interesting outcomes can be made: a number of diagnostics have poor skills, either because of a very low correlation with observations and/or because of an amplitude of the signal far from that of the observations. In contrast, a substantial number of dots lie in the portion of the diagram close to the REF line, and delimited by a correlation coefficient higher than 0.9. It appears that CNRM-CCM has a larger number of satisfactory dots than CNRM-ACM. To assess whether both model versions were statistically different, we performed a one-sample Student *t* Test to test whether the differences of the two sample means were significantly different from zero. Overall, we show that CNRM-ACM and CNRM-CCM are significantly different in most of the cases studied (see Table 1). For argument's sake, this is not the case, for example, for the equatorial temperature and water vapor at 100 hPa.

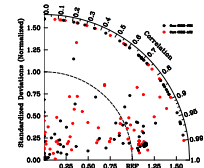


Fig. 13. Taylor diagram showing the performance of all the diagnostics of the present study for CNRM-CCM. REF line for CNRM-CCM.

Table 1. Results of the one-sample Student *t* Test to test whether the differences of the two sample means were significantly different from zero. The table shows the results for the 47-yr transient simulation (1960–2006) for the 47 diagnostics analysed in this study. The table shows the results for the 47 diagnostics analysed in this study. The table shows the results for the 47 diagnostics analysed in this study.

### 3.2 Main improvements: dynamics

Stratospheric temperature biases in spring and winter at high latitudes are smaller or comparable to those of the CCMVal-2 models (see Fig.1). and the temperature anomalies linked to volcanic eruptions follow those of the ERA-40 reanalysis (see Fig.10). The other dynamical features analysed, transition to easterlies at 60° S, strength and position of the stratospheric jets (see Fig.3) and pressure of the tropopause, compare favorably to the ERA-40 and ERA-Interim reanalyses. The characteristics of the transport appear to be quite accurately reproduced throughout the stratosphere, even though it is somewhat too rapid (see Fig.4).

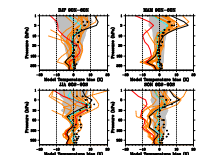


Fig. 4. Time-longitude plots of zonal wind (U) at 60° S. The plots show the transition to easterlies. The plots compare observations (black lines) with CNRM-CCM (red lines) and ERA-40 (blue lines).

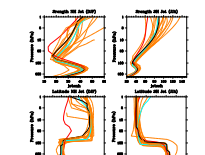


Fig. 5. Time-longitude plots of zonal wind (U) at 60° N. The plots show the transition to easterlies. The plots compare observations (black lines) with CNRM-CCM (red lines) and ERA-40 (blue lines).

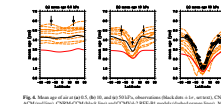


Fig. 6. Mean age of air (AOA) at 50hPa and 80hPa. The plots show AOA (days) versus latitude (lat) for observations (black lines) and CNRM-CCM (red lines).

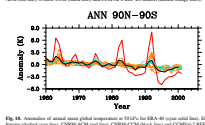


Fig. 7. Annular modes (AMs) of the zonal wind (U) at 100hPa. The plots show U (m/s) versus latitude (lat) for observations (black lines) and CNRM-CCM (red lines).

### 3.3 Main improvements: chemical species

The distributions of long-lived species, including CH<sub>4</sub> and HCl are well captured. Both the amplitude and the phase of the annual cycles of chemical species like O<sub>3</sub> and H<sub>2</sub>O are well simulated in the UTLS where the effects of transport dominate. For the several other chemical species investigated, i.e. CO, ClONO<sub>2</sub>, BrO and HNO<sub>3</sub>, the results do not reveal any major weakness in the model. Finally, our first analysis of the simulation of the ozone distribution and of the total column ozone is quite encouraging (see Fig. 11 and 18).

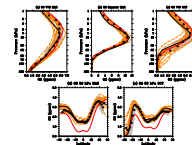


Fig. 11. Chemical species profiles (O<sub>3</sub>, H<sub>2</sub>O, CO, ClONO<sub>2</sub>, BrO, HNO<sub>3</sub>) versus altitude (hPa) for observations (black lines) and CNRM-CCM (red lines).

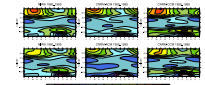


Fig. 18. Total column ozone (TCO) profiles versus latitude (lat) for observations (black lines) and CNRM-CCM (red lines).

### 3.4 Remaining weaknesses

Stratospheric temperatures are too low at the equatorial tropopause and too high in the upper stratosphere between 5 and 1 hPa warm (5 to 9 K). This warm bias extends to all latitudes, is permanent throughout the year and simulations performed with no retroaction with the chemistry onto the radiative scheme reveal that it is intrinsic to the GCM itself (see Fig.14). In the end, a number of biases appear in the chemistry of the upper stratosphere. The model produces not enough O<sub>3</sub>, but too much NO<sub>2</sub> and N<sub>2</sub>O<sub>5</sub> at 1 hPa and is then at the high end of the CCMVal-2 models (see Fig.15).

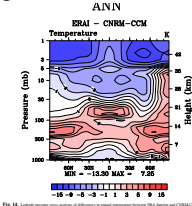


Fig. 14. Temperature profiles (K) versus altitude (hPa) for observations (black lines) and CNRM-CCM (red lines).

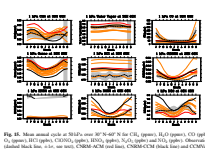


Fig. 15. Chemical species profiles (O<sub>3</sub>, H<sub>2</sub>O, CO, ClONO<sub>2</sub>, BrO, HNO<sub>3</sub>) versus altitude (hPa) for observations (black lines) and CNRM-CCM (red lines).

## 4. Future

We suggest that some of the chemical problems addressed above may be tackled by addressing issues related to the dynamics and the physics of the model. CNRM-CCM does not simulate at this stage intrinsically the QBO of the lower stratospheric equatorial winds (nor do most current CCMs). This has been identified as a major shortcoming by the CCMVal-2 project. Furthermore, the temperature of the higher stratosphere should be adjusted, possibly through the implementation of a more accurate radiation scheme in the short wavelengths. Further developments of the model will also include the non-orographic aspects of the gravity waves, as well as the short-lived source gases containing bromine. CNRM-CCM is planned for use in a variety of projects linked with the interactions between chemistry and climate, in particular in seasonal and decadal predictions, where it could possibly be coupled to an interactive ocean.